Plasmonics
DOI 10.1007/s11468-015-0053-9

Plasmonics Enhanced Average Broadband Absorption of Monolayer MoS_2

Bablu Mukherjee[1] · **Ergun Simsek**[1]

Received: 18 June 2015 / Accepted: 4 August 2015

Abstract We have studied characterization of micromechanical cleavage monolayer molybdenum disulfide (MoS_2) deposited on SiO_2/Si and glass substrates. Spherical gold (Au) nanoparticles were anchored on top of monolayer MoS_2 film. Direct reflection spectra were measured, which infers significant improvement of total average absorption of monolayer MoS_2 in Vis-NIR range of 400–800 nm by the plasmonic absorption of Au nanoparticles. Nearly 8 % average absorption was obtained in monolayer MoS_2 sample, which was increased up to 41 % by plasmonic Au nanoparticles deposited on monolayer MoS_2 film. Numerical results are also provided to describe the phenomena. This study will further add the possibilities of using layered materials in the area of solar absorption-based nano-optoelectronic devices.

Keywords Plasmonics · Nanoparticles · MoS_2 · Molybdenum disulfide · 2D materials

Introduction

Monolayer molybdenum disulfide (MoS_2) holds great promises for a range of applications among layered transition metal dichalcogenides (TMDs) due to its optical and electrical properties [1–7]. MoS_2 shows variation of optical transition depending on the atomic thickness of the film, where three distinct absorption bands corresponding to A- and B-excitons and a high-energy background peak exhibited a gradual redshift as the MoS_2 film thickness increased from the monolayer to bilayer and bulk form [8]. It is known that the scattered or absorbed field from two-dimensional (2D) atomically thin material-coated substrate can be enhanced by decorating its surface with metal nanoparticles (NPs) by surface plasmon resonance. In the past, a number of studies report that gold (Au) NP film deposition on two-dimensional active TMD layered materials for enhancing device performance and increasing Raman scattering signal [9–11]. It can be achieved that metal NPs anchored on the 2D-layered nanosheet could potentially extend its surface functionalities as better catalytic, magnetic, and optoelectronic nanomaterials [10, 12]. Various methods to fabricate TMD–nanoparticle complexes like wet method, focused laser-induced method, and thermal evaporation techniques have been employed previously [11, 13, 14]. Deposition of quantum dots or NPs on TMD nanosheet surface including MoS_2 and WSe_2 can significantly improve optical absorption, device response, scattering, and sensing properties [10, 11, 14–16]. Furthermore, attaching Au NPs on TMD can enhance photophysical properties for improved optoelectronic applications.

Mechanical exfoliation techniques have been used in an efficient way to fabricate highly crystalline thin-layered nanosheets [8, 15]. In a well-known mechanical exfoliation process, firstly thin nanosheets are separated out from their bulk using Scotch tape, where the nanosheet crystal gets cleaved on Scotch tape. Secondly, the attached thin crystals are brought in contact with the substrate and rubbed on the target substrate using a plastic tool to further cleave on the cleaned substrate [2]. In this work, we fabricated and characterized Au NP-deposited monolayer MoS_2 film. Reflection probe measurements using focused white light source was employed to acquire reflection spectra. We calculated the average absorption enhancement from reflection spectra measurements

✉ Ergun Simsek
simsek@gwu.edu

[1] Department of Electrical and Computer Engineering, School of Engineering and Applied Science, The George Washington University, Washington, DC 20052, USA

Published online: 14 August 2015

experimentally in broadband range of 400–800 nm that occurred by depositing Au NPs on surface of monolayer MoS_2. We have shown that the presence of Au NPs on the surface of monolayer MoS_2 has significantly improved the average broadband absorption. Furthermore, experimentally obtained absorption enhancement phenomena has further analyzed with the simulation results.

Results and Discussion

Mechanically exfoliated single- and few-layer MoS_2 films were deposited on 285 nm SiO_2/Si substrate. Bulk MoS_2 (SPI Supplies) was used with a piece of 3M® Brand Magic adhesive tape to fabricate different thicknesses of MoS_2 films [2]. Firstly, a small piece of bulk MoS_2 is placed in the sticky side of a piece of Scotch tape. Secondly, repeated folding and unfolding of the tape containing MoS_2 flake was performed to produce thin flakes at different parts of the tape. Lastly, the tape with different thicknesses of the flakes was gently pressed onto a cleaned SiO_2 (285 nm)/Si substrate. After few times mild rubbing with cotton-tipped wood sticks, we removed the tape from the substrate leaving behind MoS_2 flakes with different thicknesses. Atomic force microscopy (AFM) image (Fig. 1a) of a typical micromechanically exfoliated MoS_2 nanosheet, which reveals different thicknesses of layers, is combined in the nanosheet. The inset height profile along the red line of Fig. 1a determines the thickness of the nanosheet. Optical micrograph of exfoliated sample (Fig. 1b) on SiO_2/Si substrate indicates different colors from different thicknesses of the film, where the film of lowest thickness is denoted by dashed red circle. AFM image of monolayer MoS_2 film is shown in Fig. 1c, where the thickness of the film is ~0.8 nm as shown by the line profile along the red line.

Various regions of the deposited MoS_2 sample was characterized for quantitatively determining layer thickness using a confocal Raman microscopic system (Horiba Jobin-Yvon LabRam), and the Raman spectrum was collected by a ×100 objective in a backscattering geometry. The supported substrate peak at 520 cm^{-1} corresponding to mode of crystalline Si Raman band was used as standard to calibrate and optimize the signal. Two prominent peaks at ~384.5 and ~403.5 cm^{-1} were observed, which are reported to be E^1_{2g} and A_{1g} vibrational modes, respectively [2], of monolayer-thick MoS_2 prepared by micromechanical exfoliation techniques. The separation of the two main vibration modes is ~18.6 cm^{-1}, whereas the reported separation between two vibration modes is 19 and 20 cm^{-1} for mechanical exfoliated monolayer MoS_2 and CVD growth monolayer MoS_2 on SiO_2/Si substrate, respectively [4, 17].

The difference in the peak positions (Δ) indicates the number of layers in the MoS_2 nanosheet. Due to the effect of van der Waals force interaction between layers and Coulombic interlayer interaction, the difference decreases with reduction in number of layers. Bulk MoS_2 shows the energy gap (Δ) value of 26 cm^{-1} between E^1_{2g} and A_{1g} peak position, which are corresponding to in plane and out of plane vibration mode, respectively. Fabricated MoS_2 nanosheets after mechanical exfoliation exhibit different Δ-gap values (Fig. 2) of 24.9, 23.8, and 18.6 cm^{-1}, which indicates that we have achieved few-layer (NL)-, tri-layer (3L)-, and monolayer (1L)-thick MoS_2 nanosheet, respectively [5, 17].

Micromechanically exfoliated few-layer-thick MoS_2 flakes were functionalized with Au NPs (provided by Sigma-Aldrich) as shown by the scanning electron microscope (SEM) inset Fig. 3. A digital micropipette was used to drop-cast Au NP solution on MoS_2 flake on SiO_2/Si at a substrate temperature of ~120 °C in a controlled way. NPs having a diameter of ~150 nm were deposited on top of an MoS_2 sample for considering the effect of more induced dipole coupling under excitation of electromagnetic radiation [18]. MoS_2 flake with NPs was characterized using Raman spectroscopy under 532 nm laser excitation of a spot size ~1 μm in diameter. Raman spectra at two different positions as indicated by the red dashed circle A and B (inset in Fig. 3) shows that after Au NPs were placed on top of MoS_2 flake, the background counts of Raman scattering modes have increased, which could be due to the fact of plasmonic-induced enhancement of average field intensity distribution in MoS_2 flake under laser excitation [11, 18].

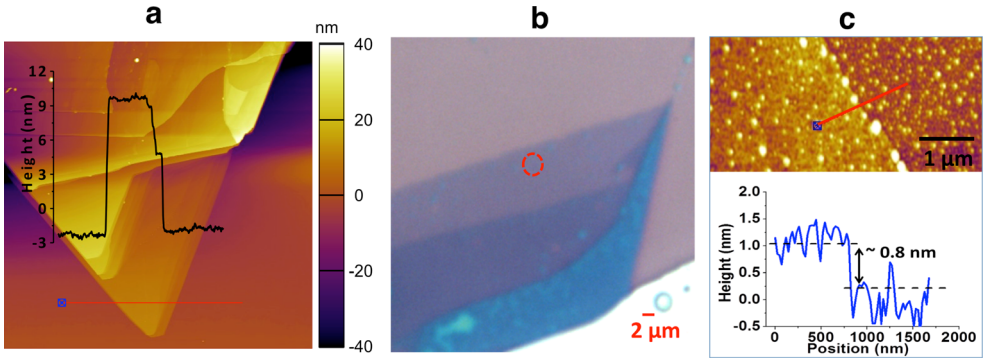

Fig. 1 **a** AFM image of mechanically exfoliated MoS_2 flake deposited on 285 nm SiO_2/Si substrate. *Inset* height profile along the *red solid line*. **b** Color optical microscopy image of a deposited MoS_2 nanosheet. *Red dashed circle* shows monolayer MoS_2 region. **c** AFM image of a single-layer (1L, thickness ~0.8 nm) MoS_2 and height profile along *red solid line*

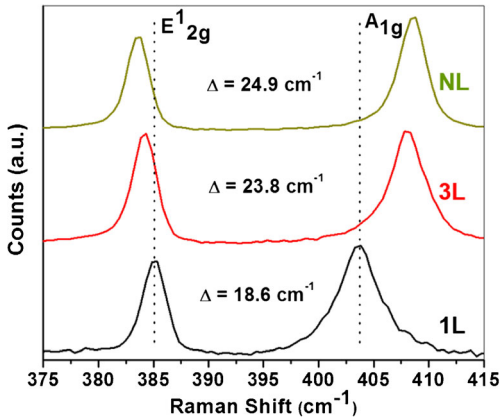

Fig. 2 Raman spectra for different thicknesses of MoS_2 nanosheet fabricated on SiO_2/Si substrate

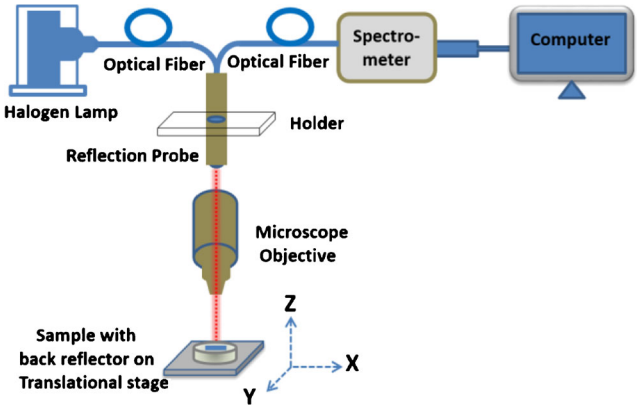

Fig. 4 Schematic of the normal incident reflection spectroscopy setup used to probe sample

To measure the reflection spectra, the spectroscopy (Fig. 4) setup was used. The white light source (halogen lamp) is fed through an optical fiber of premium-grade reflection probe (Ocean Optics). The reflection probe collects light signal at the same angle as it illuminates, which is collected by illumination fiber and read optical fiber (range: UV–Vis-NIR 300–1100 nm and core diameter 200 μm). The output signal in read fiber is connected to the spectrometer (USB 4000, Ocean Optics) with a spectrum analyzer software at a computer. In Ocean Optics SpectraSuite software, we adjusted integration time (100 ms), scans to average (10 times), and boxcar width (set 5) to maximize the signal strength and getting smooth graph. The reflection probe is attached with long working distance microscope objective lens (×20, NA 0.64) to probe the sample with focused light spot. The sample was placed on standard mirror (Thorlabs' high-quality, metal-coated optical mirrors) as broadband back reflector on XYZ-translational stage. During all measurements, the distance between microscope object and samples was kept fixed. Apart from various optical characterization tools [19, 20] of layered TMD material, this measurement setup will allow to probe the sample locally with focused white light source.

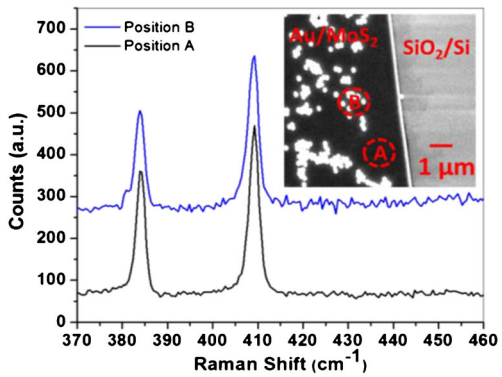

Fig. 3 Raman spectra from two different spots as indicated by a *red dashed circle* in the *inset* image. *Inset* shows SEM image of the deposited MoS_2 nanosheet with Au NPs on top

To eliminate the absorption effect of SiO_2/Si substrate, a monolayer MoS_2 sample was transferred onto quartz substrate using the technique as mentioned in [4]. Quartz substrate coated with monolayer MoS_2 with and without Au NPs was placed on top of a mirror as a back reflector on translational stage (Fig. 4). All reflection spectra were recorded using a Vis-NIR fiber spectrophotometer (USB 4000, Ocean Optics). For all reflection measurements, a standard deuterium/tungsten halogen lamp (HL-2000, Ocean Optics) was used at normal light incidence (angle of light incidence θ=90°) as a light source of illumination as shown by *source* spectrum in Fig. 5a. "Dark" spectrum (labeled in Fig. 5a) was recorded under the absence of any photon source with the lamp off or blocked, which was subtracted from each spectrum to eliminate background noise. Spectra *substrate*, *MoS_2 film*, and *Au NPs/MoS_2 film* were recorded from those respective samples as shown in Fig. 5a. We define $P_0(\lambda)$, $P_1(\lambda)$, $P_2(\lambda)$, and $P_3(\lambda)$ as direct reflection spectra of source, substrate, MoS_2 film, and Au NPs/MoS_2 film, respectively, after eliminating background intensity. The optical image (using optical microscope in transmission mode) of the sample of Au NP-deposited monolayer MoS_2 sample on quartz substrate is shown in the inset of Fig. 5b. To eliminate the contribution from the substrate as well as to correct for the spectral response of the source lamp, the absorption of monolayer MoS_2 without and with Au NPs were calculated using $(P_2(\lambda)-P_1(\lambda))/P_0(\lambda)$ and $(P_3(\lambda)-P_1(\lambda))/P_0(\lambda)$, respectively. Figure 5b shows the calculated absorption spectra of monolayer MoS_2 with and without Au NPs on the surface of the film. Two prominent peaks at ~608 and ~654 nm were observed in the calculated absorption spectra, which are known to be B and A excitonic absorption of monolayer MoS_2, respectively [18]. In the wavelength range of 400–800 nm, the monolayer MoS_2 absorbs ~8 %, whereas Au NP-deposited monolayer MoS_2 absorbs ~41 %. This does not necessarily mean that the absorption spectrum

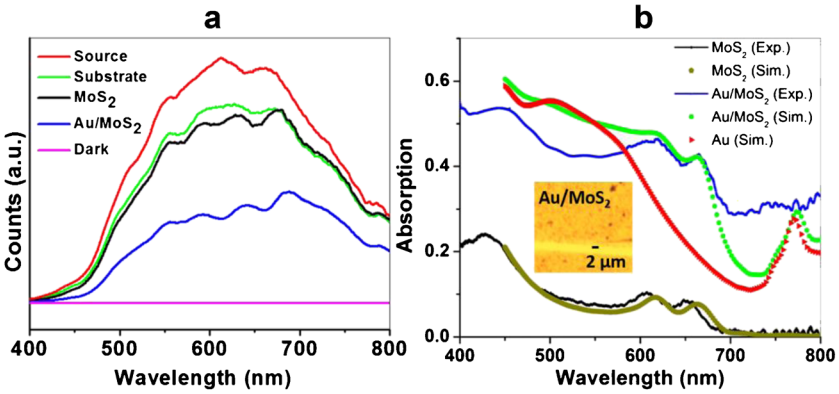

Fig. 5 **a** Relative reflection spectra from monolayer MoS_2 with and without Au NPs on top supported by quartz substrate. **b** Calculated optical absorption spectra of monolayer MoS_2 sample with and without anchored Au NPs. Simulated absorption spectra of Au NPs, monolayer MoS_2, and Au NP-coated MoS_2 in wavelength range of 450–800 nm. *Inset* shows the optical image of Au NP-deposited monolayer MoS_2 on quartz substrate

of MoS_2 is enhanced five times. However, considering the Gaussian shape of Au NPs' absorption spectra, the overall absorption spectrum of Au NP-decorated MoS_2 is not a simple addition of those two structures' (monolayer MoS_2 and Au NP array) absorption spectra. In order to verify this observation, we run a set of numerical simulations as follows.

We use Wavenology, which is a commercial finite-difference time-domain (FDTD) full-wave electromagnetic solver [21], to calculate the absorption spectra of periodically arranged Au NPs and monolayer MoS_2 with and without array of Au NP coating. The frequency-dependent permittivity of Au and MoS_2 is taken from reference [22, 23], respectively. Spherical Au NPs (diameter ~150 nm) are periodically distributed on top of a monolayer MoS_2 (thickness ~0.7 nm)-coated glass substrate. The refractive index of glass is assumed to be 1.5. The inter-nanoparticle spacing is 285 nm along the *x*- and *y*-axes. In the simulation unit, two different monitors at reflection and transmission geometry are used to collect the spectra, which results in the simulated spectra (Fig. 5b) using the formula of absorption, which is equivalent to 1—reflection–transmission. In Fig. 5b, the simulated results of Au NP array, monolayer MoS_2, and MoS_2 with coating of Au NP array are plotted with the experimental results. There are three important points. First, the absorption spectra of monolayer MoS_2 obtained by experiment and simulation are matched reasonably well. Second, the absorption spectrum of Au NP array shows a Gaussian-like behavior as expected. Third, and most importantly, the absorption spectrum of Au NP-decorated MoS_2 is not equal to the addition of Au NP's and MoS_2's individual absorption spectra. It is evident that for the wavelengths between 550 and 750 nm, excitonic and plasmonic absorption of MoS_2 and Au NPs, respectively, enhance each other. Note that the Au NPs were not periodically aligned in the experiment, and hence, a discrepancy exists between the experimental and simulation results of the absorption spectra of Au nanoparticle-coated MoS_2 sample.

Conclusion

To sum up, Au nanoparticle-decorated monolayer MoS_2 samples were fabricated and characterized. Average absorption was calculated from experimentally recorded reflection spectra, which was further analyzed using FDTD simulation results. We obtained the average (%) absorption of around five times higher at a wavelength range of 400–800 nm after depositing Au NPs on the surface of monolayer MoS_2 by locally probing the sample with focused white light illumination.

References

1. Novoselov KS (2011) Nobel lecture: graphene: materials in the Flatland. Rev Mod Phys 83:837–849
2. Li H, Wu J, Yin Z, Zhang H (2014) Preparation and applications of mechanically exfoliated single-layer and multilayer MoS_2 and WSe_2 nanosheets. Acc Chem Res 47:1067–1075
3. Xia F, Wang H, Xiao D, Dubey M, Ramasubramaniam A (2014) Two-dimensional material nanophotonics. Nat Photonics 8:899–907
4. Mukherjee B, Tseng F, Gunlycke D, Amara KK, Eda G, Simsek E (2015) Complex electrical permittivity of the monolayer molybdenum disulfide (MoS_2) in near UV and visible. Opt Mater Express 5(2):447–455
5. Ye M, Winslow D, Zhang D, Pandey R, Yap YK (2015) Recent advancement on the optical properties of two-dimensional molybdenum disulfide (MoS_2) thin films. Photonics 2:288–307
6. Eda G, Yamaguchi H, Voiry D, Fujita T, Chen M, Chhowalla M (2011) Photoluminescence from chemically exfoliated MoS_2. Nano Lett 11:5111–5116
7. Chhowalla M, Shin HS, Eda G, Li LJ, Loh KP, Zhang H (2013) The chemistry of two-dimensional layered transition metal dichalcogenide nanosheets. Nat Chem 5:263–275
8. Dhakal KP, Duong DL, Lee J, Nam H, Kim M, Kan M, Lee YH, Kim J (2014) Confocal absorption spectral imaging of MoS_2: optical transitions depending on the atomic thickness of intrinsic and chemically doped MoS_2. Nanoscale 6:13028–13035

9. Lin J, Li H, Zhang H, Chen W (2013) Plasmonic enhancement of photocurrent in MoS_2 field-effect-transistor. Appl Phys Lett 102: 203109
10. Shi Y, Huang JK, Jin L, Hsu YT, Yu SF, Li LJ, Yang HY (2013) Selective decoration of Au nanoparticles on monolayer MoS_2 single crystals. Sci Rep 3:1839
11. Mukherjee B, Leong WS, Li Y, Gong H, Sun L, Shen ZX, Simsek E, Thong JTL (2015) Raman analysis of gold on WSe_2 single crystal film. Mat Res Exp 2:065009
12. Huang X, Zeng Z, Bao S, Wang M, Qi X, Fan Z, Zhang H (2013) Solution-phase epitaxial growth of noble metal nanostructures on dispersible single-layer molybdenum disulfide nanosheets. Nat Commun 4:1444
13. Cao W, Pankratov V, Huttula M, Shi X, Saukko S, Huang Z, Zhang M (2015) Gold nanoparticles on MoS_2 layered crystal flakes. Mater Chem Phys 158:89–95
14. Lu J, Lu JH, Liu H, Liu B, Gong L, Tok ES, Loh KP, Sow CH (2015) Microlandscaping of Au nanoparticles on few-layer MoS_2 films for chemical sensing. Small 11(15):1792–1800
15. Sreeprasad TS, Nguyen P, Kim N, Berry V (2013) Controlled, defect-guided, metal-nanoparticle incorporation onto MoS_2 via chemical and microwave routes: electrical, thermal, and structural properties. Nano Lett 13(9):4434–4441
16. Kufer D, Nikitskiy I, Lasanta T, Navickaite G, Koppens FHL, Konstantatos G (2015) Hybrid 2D–0D MoS_2–PbS quantum dot photodetectors. Adv Mater 27:176–180
17. Lee C, Yan H, Brus LE, Heinz TF, Hone J, Ryu S (2010) Anomalous lattice vibrations of single- and few-layer MoS_2. ACS Nano 4(5):2695–2700
18. Mertens J, Shi Y, Sanchez AM, Wirtz L, Yang HY, Baumberg JJ (2014) Excitons in a mirror: formation of "optical bilayers" using MoS_2 monolayers on gold substrates. Appl Phys Lett 104:191105
19. Yim C, O'Brien M, McEvoy N, Winters S, Mirza I, Lunney JG, Duesberg GS (2014) Investigation of the optical properties of MoS_2 thin films using spectroscopic ellipsometry. Appl Phys Lett 104: 103114
20. Mak KF, He K, Shan J, Heinz TF (2012) Control of valley polarization in monolayer MoS_2 by optical helicity. Nat Nanotechnol 7: 494–498
21. Wavenology from Wave Computation Technologies, Inc., Durham, NC
22. Palik ED (1997) Handbook of optical constants of solids. Elsevier Inc.
23. Li Y, Chernikov A, Zhang X, Rigosi A, Hill HM, van der Zande AM, Chenet DA, Shih EM, Hone J, Heinz TF (2014) Measurement of the optical dielectric function of monolayer transition-metal dichalcogenides: MoS_2, $MoSe_2$, WS_2, and WSe_2. Phys Rev B 90: 205422